Hybrid Integration of a Single-Frequency Ring Laser with a Microelectronic Driver

Stanisław Stopiński, Krzysztof Siwiec, Witold Pleskacz, Sławomir Szostak, Ryszard Kisiel and Ryszard Piramidowicz
Warsaw University of Technology, Institute of Microelectronics and Optoelectronics, Koszykowa 75, 00-662 Warsaw, Poland
e-mail:stanislaw.stopinski@pw.edu.pl

ABSTRACT

In this work a concept of hybrid integration of a photonic integrated circuit with an integrated microelectronic driver is demonstrated. The idea is based on the flip-chip technique and is discussed using an example of a single frequency ring laser, realized in the framework of development of an optical gyroscope system. The laser is monolithically integrated with a detection circuit of the beating signal between two counter-propagating modes, resulting from the Sagnac shift. Initial characterization results of the fabricated laser confirm single frequency operation with the output power on the order of 1 mW within the cavity and side mode suppression ratio over 35 dB. The measured imbalance between the power level of the modes is ca. 10 dB, which can be compensated by optical amplifiers implemented in the detection circuit.

Keywords: application specific photonic integrated circuit, generic integration technology, application specific integrated circuit, hybrid integration, flip-chip technology, ring laser gyroscope.

1. INTRODUCTION

In recent years photonic integration technologies have been extensively developed with a specific attention given to telecom and sensing applications, where multiple channel operation is highly advantageous in comparison to traditional solutions based on discrete photonic devices. However, despite excellent performance in the laboratory environment, nowadays very few large-scale integrated devices are offered on a commercial basis. One of the major problems is lack of an efficient and scalable technique for integration of multiple high-speed active photonic components, i.e. lasers, modulators and detectors, with microelectronic drivers. A typical scheme of bonding, when the photonic chip is positioned next to the electronic circuits, may result in long bondwires and thus also high inductance of such an electrical connection. This, in turn, hampers the RF performance of complete optoelectronic systems. On the other hand, designing dedicated RF micro-strip lines or coplanar waveguides on the surface of the photonic chip sacrifices too much of its area. A hybrid integration scheme proposed in this work could be an efficient technique of connecting integrated microelectronic drivers with multiple high-speed active components of photonic integrated circuits.

The discussed concept is based on the flip-chip technique and will be presented using an example of a single-frequency ring laser, realized in the framework of development of a fully integrated optical gyroscope system. Up to date ring laser gyroscopes (RLGs) [1] are typically constructed using helium neon or solid state lasers, due to excellent spectral properties of the generated beams [2]. Such systems have proven excellent performance as rotation sensors in top-class inertial measurement units (IMUs) mounted in airplanes, spacecrafts and missiles. Integration of a gyroscope system remains a technological challenge, as it requires sufficiently good spectral properties (single frequency operation and a narrow laser line) combined with a relatively large ring perimeter (on the order of 10 mm). In this work we demonstrate a novel, proof-of-concept electronic-photonic hybrid system. It comprises an application specific photonic integrated circuit (ASPIC) providing combined functionality of a bi-directional single-frequency ring laser source and a detection circuit of the beating signal. The layout of the device is compatible with a dedicated microelectronic driver developed in parallel.

2. ASPIC DESIGN

Single-frequency integrated ring lasers in the indium phosphide technology can be realized using e.g. arrayed waveguide gratings (AWGs) or asymmetric Mach-Zehnder interferometers (AMZIs) as intra-cavity wavelength filters [3-7]. The latter solution provides tunability and precise control over the generated wavelength of the laser and thus also enable optimizing its output power by adjusting it to the maximum of the amplifier gain curve. An operational scheme of the designed photonic circuit is presented in Figure 1a.

A semiconductor optical amplifier (SOA 1) is the gain section of the laser. A cascade of three wavelength filters, each with a different value of free spectral range (70 nm, 5.8 nm and 0.56 nm) enables single frequency operation. The filters comprise two 1×2 multi-mode interference (MMI) splitters/combiners and two electro-optic phase modulator (EOPM) sections, which allow to accurately tune the maxima of the transmission bands of all filters to the same wavelength. Thus, the output power and side mode suppression ratio of the laser line could be optimized. Figure 1b presents the effective power transmission characteristic of the cascade of all three filters connected in series.

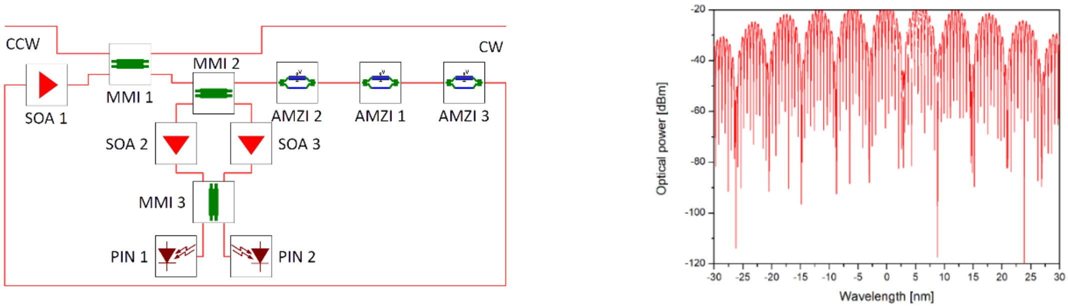

Figure 1. a) Operational scheme of the single-frequency ring laser system;
b) Power transmission characteristic of a cascade of three asymmetric Mach-Zehnder interferometers.

The laser design enables bi-directional operation, i.e. both clockwise (CW) and counter-clockwise (CCW) modes can be generated simultaneously. The Sagnac effect, occurring under rotation of the optical chip with the angular velocity Ω, will cause a split of the CW and CCW resonant frequencies ν (which is the same at rest for both modes) by $\Delta\nu$, following equation (1): $\Delta\nu = (4a\nu\Omega)/(pc)$, where a is the area of the cavity and p its perimeter. The frequency difference can be read out by monitoring the beating signal of the two laser modes. The CW and CCW signals are coupled out of the cavity using a 2×2 MMI (MMI 2) coupler and interfere at the output of a second 2×2 MMI (MMI 3). Since typically one mode has a higher power than the second one, two SOA sections are introduced to balance their power level. Two PIN photodiodes are connected to the outputs of MMI 3, which enables monitoring of the beating signal being a result of interference of CW and CCW laser mode.

3. ASIC DESIGN

The microelectronic driver of the RLG system was realized as an application specific integrated circuit (ASIC). The device is used to power the amplifiers of the ring laser and the detection circuit (forward bias applied by controlled current sources) and tune the phase shift introduced by electro-optic modulators of the AMZIs (reverse bias applied by controlled voltage sources).

Furthermore, the ASIC is used to read out the photocurrent of the PIN photodiodes and perform basic processing of the recorded signals. The readout circuit comprises a programmable transimpedance amplifier (TIA) and a comparator. The TIA converts and amplifies the current signal from the photodiodes. The TIA has a programmable gain from 300 V/A to 2.4 kV/A with a 6 dB step. Additionally the TIA can compensate input bias current within the range from 250 µA to 8 mA. The digital part of the ASIC comprises configuration registers and a frequency detector, which compares the frequency at the AFE output with a reference clock signal.

4. MASK LAYOUT

The ASPIC layout has been designed using the generic technology provided by SMART Photonics in the framework of multi-project wafer runs [8, 9], offering access to amplifiers, electro-optic phase modulators, PIN photodiodes and passive waveguides. The ASIC driver has been implemented and prototyped in the AMS 0.35 µm technology. Mask layout of both devices is presented in Figure 2.

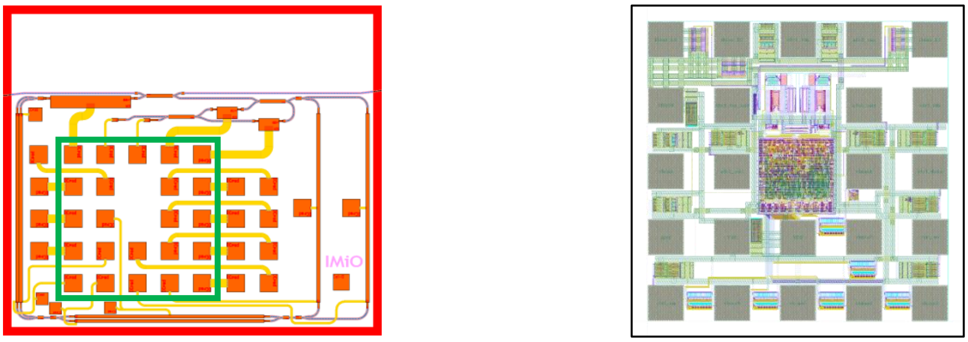

Figure 2. a) Mask layout of the single-frequency ring laser integrated with a beating signal detection circuit;
b) Mask layout of the microelectronic driver.

The laser gain section has the length of 1 mm. On the left-hand side it is connected to a cascade of three AMZI filters, with the length imbalance Δl_2 = 119 µm, Δl_1 = 12 µm and Δl_3 = 1252 µm, respectively. The output of the third AMZI is connected to the MMI 2, which couples the CW and CCW from of the laser cavity to the detection circuit, which comprises the amplifiers SOA 2 and SOA 3 (both having the length of 250 μm), MMI 3 coupler and two PIN photodiodes. Furthermore, an additional 2×2 MMI (MMI 1 in Figure 1a) is introduced within the cavity, which enables performing optical characterization of the fabricated chip both for the CW and CCW mode. The total resonator length is around 14 mm, rectangular shape was chosen to maximize the area of laser and thus increase the gyroscope scale factor (see equation 1). The circuit size is 4.6 mm × 2.9 mm, it intentionally uses only a part of a standard SMART Photonics MPW cell.

Both devices have been designed taking into account further flip-chip bonding procedure. The green square in Figure 2a, with the dimensions of 2.0 mm × 2.0 mm equal to the ASIC size, indicates the area, where the driver will be flip-chip bonded. All of the bonding pads have the size of 220 μm × 220 μm. Eleven pads are used to connect the ASIC with the ASPIC active components (three SOAs, six EOPMs and two photodiodes). Furthermore, twelve pads are used to provide the ASIC with the power supply and control signals through electrical tracks on the ASPIC.

5. CHARACTERIZATION RESULTS

After the fabrication the ring laser circuit has been optically characterized. Figure 3a presents the emission spectra, recorded using a high-resolution optical spectrum analyser, for CW and CCW modes, obtained after careful adjusting the transmission of all three interferometers. The measured lasing wavelength is 1554.5 nm and the side mode suppression ratio over 35 dB for both modes, which confirms single-frequency operation. Figure 3b presents the recorded fiber-coupled power characteristic as a function of the SOA injection current. Since the signals within the cavity are ca. 3-4 dB higher, as they do not suffer from the chip-fiber coupling loss, it can be concluded that the obtained power levels on the order of 0.3-1.0 mW are sufficient for proper operation of a gyroscope system. The imbalance between the modes for the SOA driving current between 75 mA and 150 mA does not exceed 10 dB, which means that it can be easily compensated by the amplifiers in the detection circuit.

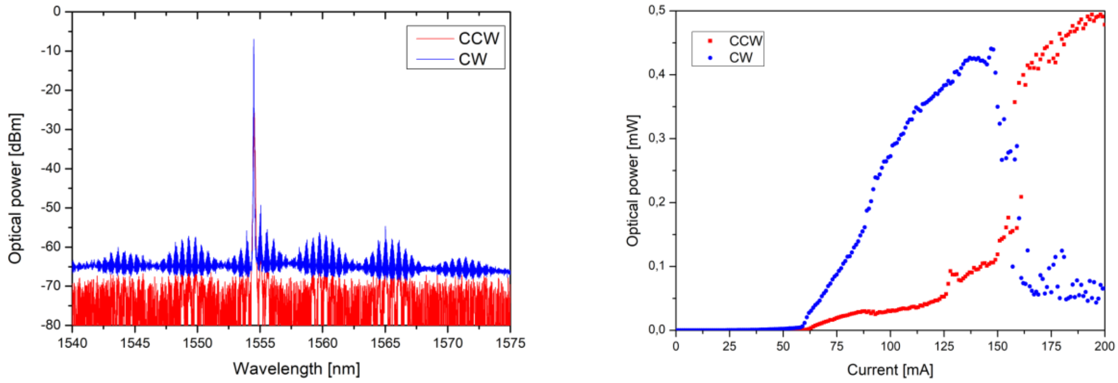

Figure 3. a) Emission spectrum of the single frequency ring laser measured for both modes using high-resolution optical spectrum analyser; b) Measured LI characteristics of the laser for both modes.

6. SUMMMARY

A concept of hybrid integration of a single-frequency ring laser system with a dedicated integrated microelectronic driver has been presented and discussed. The obtained results are promising with respect to application of such an approach in further development of a fully integrated optical gyroscope.

ACKNOWLEDGEMENTS

The research leading to these results has received funding from the National Science Centre (decision DEC-2013/09/N/ST7/04430) and from the EU Horizon 2020 research and innovation programme under grant agreement No. 687777 (PICs4All).

REFERENCES

[1] W. M. Macek, D. T. M. Davis, “Rotation rate sensing with traveling-wave ring lasers,” Appl. Phys. Lett., vol. 2, no. 3, pp. 67–68, 1963.
[2] M. N. Armenise, Advances in Gyroscope Technologies. Berlin, Germany: Springer-Verlag, 2010.
[3] S. Latkowski et al., “Monolithically integrated widely tunable laser source operating at 2 μm”, Optica 3, 1412-1417 (2016)
[4] J. H. den Besten et al., “A compact digitally tunable seven-channel ring laser,” IEEE Photon. Technol. Lett., vol. 14, no. 6, pp. 753–755, Jun. 2002.
[5] B. W. Tilma et al., “Integrated tunable quantum-dot laser for optical coherence tomography in the 1.7 μm wavelength region,” IEEE J. Quantum Electron., vol. 48, no. 2, pp. 87–98, Feb. 2012.
[6] S. Latkowski et al., “Novel widely tunable monolithically integrated laser source,” IEEE Photon. J., vol. 7, no. 6, pp. 1–9, Dec. 2015.
[7] S. Stopinski, L. Augustin and R. Piramidowicz, "Single-Frequency Integrated Ring Laser for Application in Optical Gyroscope Systems," IEEE Photonics Technology Letters, vol. 30, no. 9, pp. 781-784, 1 May1, 2018.
[8] M. Smit et al., “An introduction to InP-based generic integration technology,” Semicond. Sci. Technol., vol. 29, no. 8, p. 083001, 2014.
[9] SMART Photonics website, http://smartphotonics.nl/fsfsd